PROCEEDINGS of the
23rd International Congress on Acoustics
9 to 13 September 2019 in Aachen, Germany

Characterization of the aeroacoustic instability in a T-junction

Claire BOURQUARD[1], Abel FAURE-BEAULIEU[1], Nicolas NOIRAY[1]

[1]CAPS Laboratory, Department of Mechanical and Process Engineering, ETH Zürich, 8092 Zürich, Switzerland

Abstract

Aeroacoustic resonance at a T-junction is a well-known phenomenon that has been studied using a variety of different approaches. These include vortex-sheet modelling of the shear layer and Linearised Navier-Stokes Equations (LNSE) incorporating a turbulence model. The aeroacoustic instability results from the constructive interaction of the acoustic waves in the cavity and the turbulent shear layer. In the present study, measurements of the acoustic impedance of the shear layer and of the cavity are performed at different frequencies and mean flow velocities. These measurements are used to derive a linear model of the aeroacoustic instability and allow for analysis of linear stability.

Keywords: Aeroacoustics, Linear model, Impedance

1 INTRODUCTION

Flow past the opening of a closed side-branch, as for example performed in a T-junction, is of great concern in a wide variety of practical applications such as ducts, pipe and ventilation systems or even wind instruments, since the coupling between the acoustic waves in the closed branch and the turbulent shear layer can result in aeroacoustic resonance. This phenomenon has been the subject of multiple studies since more than 50 years, beginning with wind tunnel experiments and first empirical models [8, 1, 10]. In later studies, more detailed modelling of the shear layer was performed by using vortex-sheet theory [7, 5]. Latest studies include numerical simulations to discuss the influence of the cavity edges on the generation mechanism [4], thorough experimental investigations [6] and instability modelling using Linearised Navier-Stokes Equations (LNSE) incorporating a turbulence model [2]. The present study aims at bridging a simple analytical model of two coupled oscillators with the experiments performed on a rectangular T-junction.

In a first part, the analytical model used for modelling the T-junction aeroacoustic resonance will be derived. In a second part, the experimental campaign will be described. In the last part, the results of the model with fitted parameters will be compared with the full T-junction aeroacoustic experiments.

2 ANALYTICAL MODEL

2.1 Acoustic-hydrodynamic coupled system

The configuration considered in the present study consists in a turbulent air flow of mean velocity U running through a channel of square cross section with a perpendicular side branch of rectangular cross section, and whose depth L can be manually adjusted with a piston. A sketch of the system can be seen in Fig. 1. Since the fluid in the side-branch is quiescent, a turbulent shear layer forms between the main channel and the side branch. Depending on the mean flow velocity U and the side-branch length L, constructive feedback can be achieved between the acoustic waves travelling inside the side branch and the shear layer, resulting in an aeroacoustic instability. For the model, the system will be divided in two coupled subsystems: the side branch on the one side, and the shear layer on the other side, coupled at the reference plane $y = 0^-$. The side branch is modelled as a damped acoustic oscillator, following the quarter-wave resonator modelling of [3]. We note $\tilde{u}$ the acoustic velocity in m/s and $u = \rho c \tilde{u}$ the "normalized" acoustic velocity in Pa. With this, the specific admittance of the side branch at reference plane $y = 0^-$ can be expressed in the frequency domain as follows:

[1]clairebo@ethz.ch, noirayn@ethz.ch

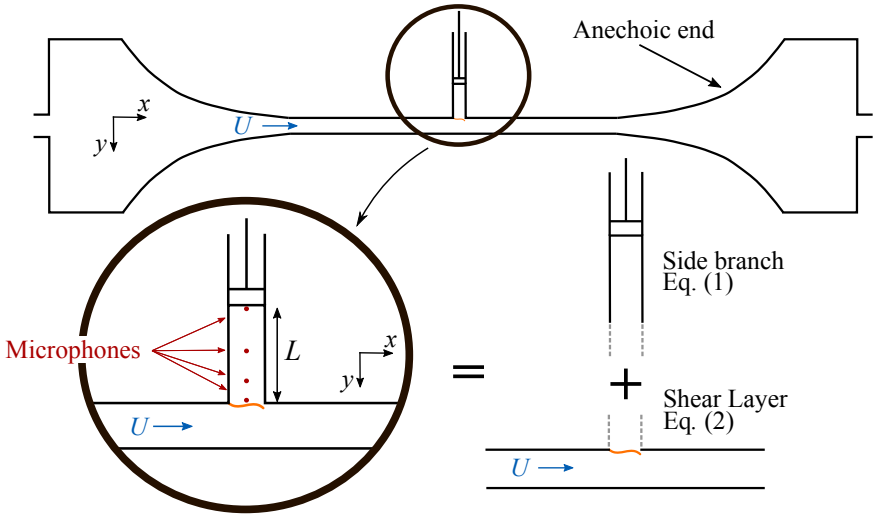

Figure 1. Sketch of the resonant T-junction system, divided into separate acoustical elements : side branch (Eq. 1) and shear layer (Eq. 2). Please note that the shear layer element also includes the area expansion, which means that the response of this element will be a mix of acoustic and hydrodynamic response.

$$A_P(s) = \frac{\hat{u}}{\hat{p}} = -\frac{\gamma s}{s^2 + 2\alpha s + \omega_a^2}, \tag{1}$$

with p the acoustic pressure, $s = i\omega$ the Laplace variable, and ω is the varying angular frequency. α is the damping, γ represents the inverse of the effective mass of the oscillator, and ω_a is the resonance angular frequency of the side branch. The value of the parameters α, γ, and ω_a depends on the side branch length L. The subscript "a" stands for "acoustic", since we will label the side branch subsystem as the "acoustic oscillator". A higher level of complexity was needed to capture the acoustic response of the shear layer, which is why in this case a transfer function of order 2 was used for the specific impedance as follows:

$$Z_{SL}(s) = \frac{\hat{p}}{\hat{u}} = G\frac{s^2 + 2ds + \omega_0^2}{s^2 + 2bs + \omega_h^2}, \tag{2}$$

with G, b, d, and frequencies ω_0 and ω_h depending on the mean flow velocity U and to be determined from the fit in the next section. In reality, this subsystem entails the shear layer as well as the expansion from the side branch to the channel. For this reason, it is a mix of acoustic and hydrodynamic response. However, for the sake of simplicity, this subsystem will be labelled as the "hydrodynamic oscillator", which is why the subscript "h" is used, standing for "hydrodynamic". Using the two previously defined subsystems, the coupled system in time domain becomes:

$$\begin{cases} \ddot{u} + 2\alpha\ \dot{u} + \omega_a^2\ u = -\gamma\ \dot{p} \\ \ddot{p} + 2b\ \dot{p} + \omega_h^2\ p = G(\ddot{u} + 2d\ \dot{u} + \omega_0^2\ u), \end{cases} \tag{3}$$

Using the first equation to express the second derivative of the acoustic velocity $\ddot{u}$, the system can be rewritten:

$$\begin{cases} \ddot{u} + 2\alpha\ \dot{u} + \omega_a^2\ u = -\gamma\dot{p} \\ \ddot{p} + 2\beta\ \dot{p} + \omega_h^2\ p = \mu\dot{u} + \lambda u, \end{cases} \tag{4}$$

With $\beta = (2b + G\gamma)/2$, $\mu = 2G(d - \alpha)$ and $\lambda = G(\omega_0^2 - \omega_a^2)$. The original system was now reduced to a simple coupled system of damped harmonic oscillators with a mix of dissipative and reactive coupling.

2.2 Stability

The system can be written in matrix form using $x = \begin{pmatrix} u \\ p \end{pmatrix}$:

$$\underbrace{\begin{bmatrix} 1 & 0 \\ 0 & 1 \end{bmatrix}}_{M} \ddot{x} + \underbrace{\begin{bmatrix} 2\alpha & \gamma \\ -\mu & 2\beta \end{bmatrix}}_{D} \dot{x} + \underbrace{\begin{bmatrix} \omega_a^2 & 0 \\ -\lambda & \omega_h^2 \end{bmatrix}}_{K} x = 0. \tag{5}$$

Thus, the stability of this linear system depends on the sign of is eigenvalues, which are the roots of:

$$\det(s^2 M + sG + K) = (s^2 + 2\alpha s + \omega_a^2)(s^2 + 2\beta s + \omega_h^2) + \gamma s(\mu s + \lambda) = 0. \tag{6}$$

The characteristic polynomial of the system is:

$$s^4 + s^3 2(\alpha + \beta) + s^2(\omega_a^2 + \omega_h^2 + 4\alpha\beta + \gamma\mu) + s(2\alpha\omega_h^2 + 2\beta\omega_a^2 + \gamma\lambda) + \omega_a^2\omega_h^2. \tag{7}$$

The roots of this polynomial correspond to the eigenvalues of the coupled system, which will be compared to the spectrum of the aeroacoustic instability for different velocities in Section 4.

3 EXPERIMENTS

3.1 Aeroacoustic resonance

The system considered in the present study consists of a 62x62 mm^2 channel about 2m long, crossed by a flow of mean velocity U varied between 35 and 75 m/s. In the middle of the channel, a side branch of length L (varied between 0 and 380mm with a piston) and of cross section 62x30mm^2 is connected to the main channel via a sharp-edged perpendicular T-junction. For the rest of the study, we fix the side branch length at $L = 250$ mm. As can be seen in Fig. 1, four G.R.A.S. 46BD 1/4" CCP microphones are installed inside the side branch. The pressure at the fourth microphone, at the end of the side branch, is measured for different velocities, varying from 35 to 75 m/s. The results in terms of spectrum is shown in Fig. 2.

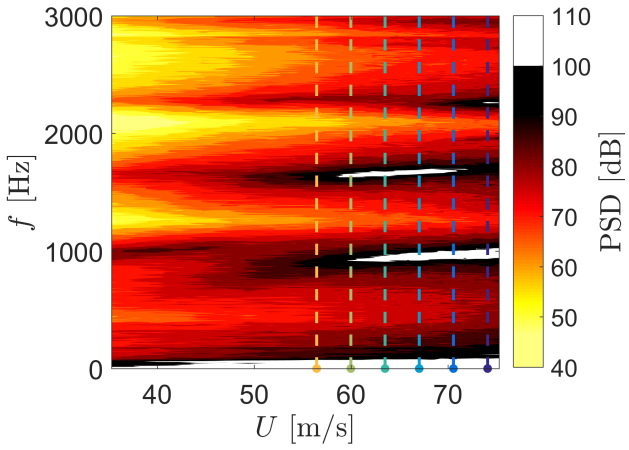

Figure 2. Acoustic mapping of the shear layer - side branch T-junction aeroacoustic resonance in terms of Power Spectral Density (PSD) for different mean flow velocities U for $L = 250$mm. The spectra for chosen velocities (colored dashed lines) will be compared to the fitted model in Section 4.

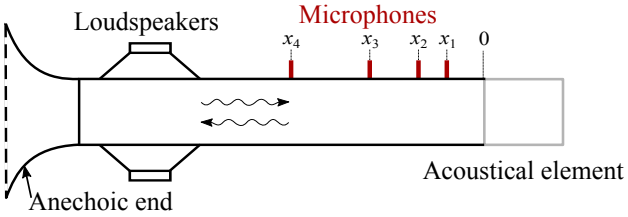

Figure 3. Sketch of the impedance tube used for the subsystems reflection coefficient measurements

3.2 Identification of the model parameters

For the determination of the parameters in Eqs. 1 and 2, the acoustic response of the side branch on the one side, and of the shear layer on the other side, is measured. For this purpose, reflection coefficient measurements are performed using the multi-microphone method (MMM) [9] in an impedance tube of 62x30 mm^2 cross-section, equipped with 2 Beyma CP850Nd compression drivers facing each other, and 4 (for the side branch) or 6 (for the shear layer) G.R.A.S. 46BD 1/4" CCP microphones. On the microphone side end of the impedance tube, the acoustic element to be measured is placed (in the present case, either the side branch or the expansion + shear layer from Fig. 1). On the loudspeaker side end of the impedance tube, an anechoic end is installed, which prevents acoustic waves reflection. A sketch of the experimental setup can be seen in Fig. 3.

Once the reflection coefficient has been measured, the specific impedance can be obtained using $Z = (R-1)/(R+1)$, and the specific admittance $A = 1/Z$. Following this, the measurements can be fitted using Eqs. 1 and 2. The results of the measurements and fits can be found in Fig. 4.

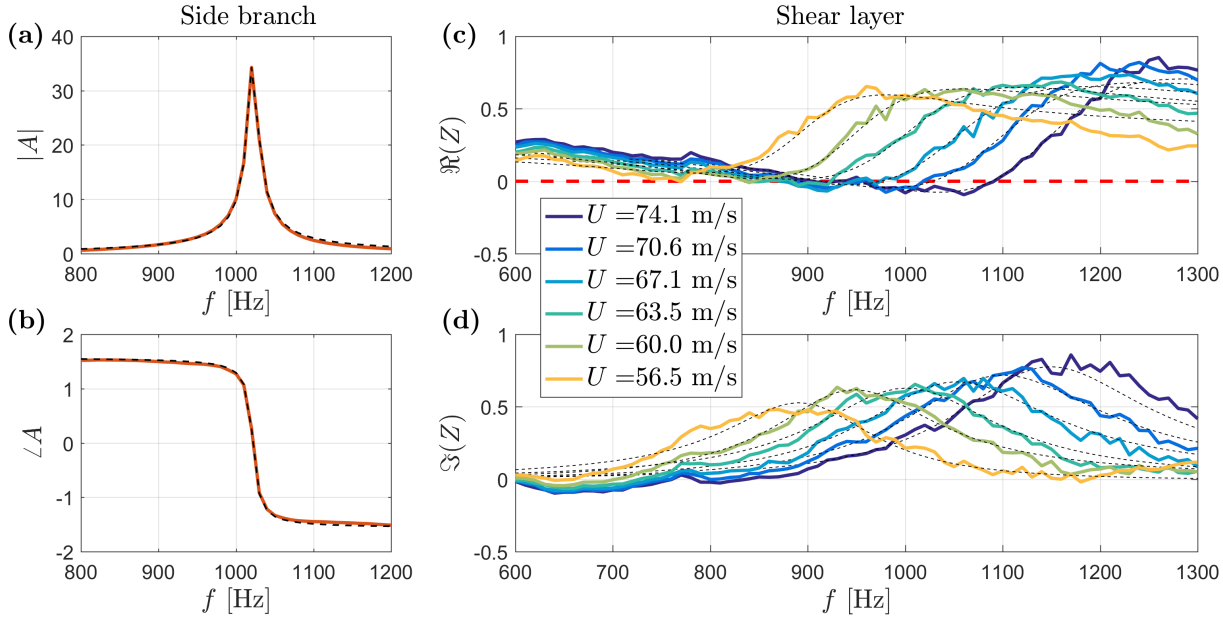

Figure 4. **(a)** and **(b)**: modulus and phase of the specific admittance of the side branch for $L = 250$ mm from MMM measurements. The black dashed line corresponds to the fit based on Eq. 1. **(c)** and **(d)**: real and imaginary part of the shear layer impedance for low excitation amplitude and different velocities U. The black dashed lines correspond to the fit based on Eq. 2. Please note the range of frequencies for which $\Re(Z) < 0$, which means that the shear layer amplifies disturbances in this region and might lead to an instability.

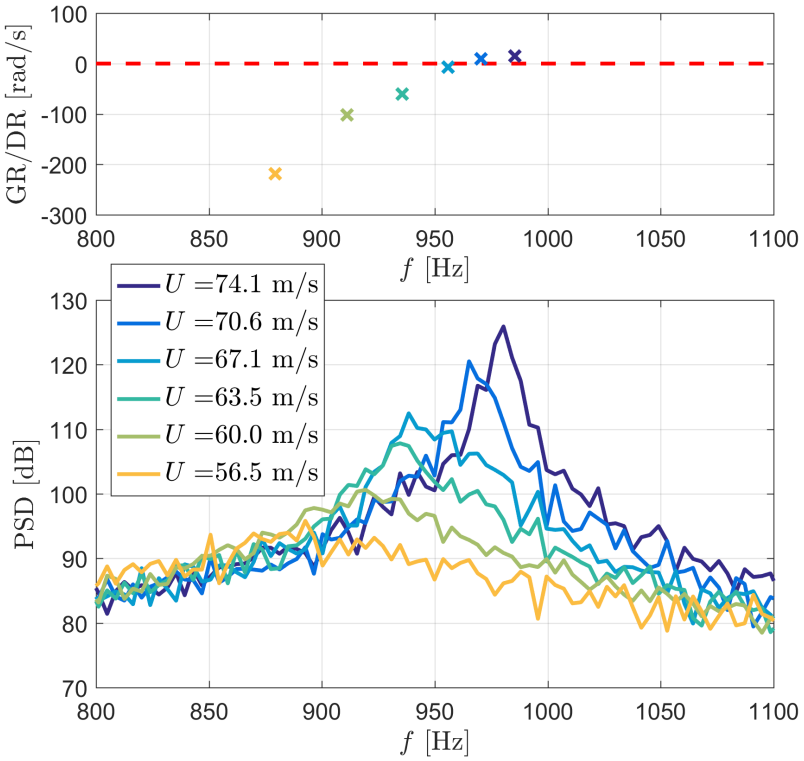

Figure 5. Most unstable eigenvalue of the coupled system for varying mean flow velocity U through the channel (top). Spectra of the aeroacoustic coupled system for the same velocities (bottom), corresponding to the colored dashed lines in Fig. 2.

4 COMPARISON OF THE EXPERIMENTS WITH THE FITTED MODEL

The eigenvalues of the fitted model can now be compared with the frequency response of the experimental coupled system. This comparison between the most unstable eigenvalue of the fitted model (i.e. the one with the highest real part) and the experimental spectra from Fig. 2 is shown in Fig. 5. The imaginary part of the model eigenvalues corresponds to the frequency of the mode, which is in excellent agreement with the frequency of the highest peak in the spectra. For $U = 74.1$ and $U = 70.6$ m/s, the modelled system has an eigenvalue whose real part is positive, meaning that the system is unstable. In the experimental power spectral density (PSD), the instability is characterized by a sharp peak, which underlines the good agreements between fitted model and experiments in terms of stability.

5 CONCLUSIONS

In the present study, the aeroacoustic resonance of a T-junction coupling a shear layer and a side branch was studied. For this purpose, the frequency response of the coupled system was measured at different mean flow velocities U. Then, the acoustic admittance and impedance of the two subsystems (side branch and shear layer) were measured separately by the multi-microphone method. An analytical model was derived for the admittance of the side branch and for the impedance of the shear layer, which parameters could be fitted on the previous measurements. The eigenvalues of the fitted coupled system were in very good agreement with the experimental spectra of the aeroacoustic instability, both in terms of frequency and stability.

REFERENCES

[1] A. J. Bilanin and E. Covert. Estimation of possible excitation frequencies for shallow rectangular cavities. AIAA journal, 11(3):347–351, 1973.

[2] E. Boujo, M. Bauerheim, and N. Noiray. Saturation of a turbulent mixing layer over a cavity: response to harmonic forcing around mean flows. Journal of Fluid Mechanics, 853:386–418, 2018.

[3] C. Bourquard and N. Noiray. Stabilization of acoustic modes using helmholtz and quarter-wave resonators tuned at exceptional points. Journal of Sound and Vibration, 445:288–307, 2019.

[4] S. Dequand, S. Hulshoff, and A. Hirschberg. Self-sustained oscillations in a closed side branch system. Journal of Sound and Vibration, 265(2):359–386, 2003.

[5] M. S. Howe. Acoustics of fluid-structure interactions. Cambridge university press, 1998.

[6] M. Karlsson and M. Åbom. Aeroacoustics of t-junctions—an experimental investigation. Journal of Sound and Vibration, 329(10):1793–1808, 2010.

[7] M. Peters and H. Hoeijemakers. A vortex sheet method applied to unsteady flow separation from sharp edges. Journal of Computational Physics, 120(1):88–104, 1995.

[8] J. Rossiter. Wind tunnel experiments on the flow over rectangular cavities at subsonic and transonic speeds. Technical report, Ministry of Aviation; Royal Aircraft Establishment; RAE Farnborough, 1964.

[9] B. Schuermans, V. Bellucci, F. Guethe, F. Meili, P. Flohr, and C. O. Paschereit. A detailed analysis of thermoacoustic interaction mechanisms in a turbulent premixed flame. In Proc. ASME Turbo Expo 2004, volume 1, pages 539–551, 2004.

[10] C. K. Tam and P. J. Block. On the tones and pressure oscillations induced by flow over rectangular cavities. Journal of Fluid Mechanics, 89(2):373–399, 1978.